scientific reports

Check for updates

OPEN

Phytobacter sp. RSE02 is a rice seed endophytic plant probiotic bacterium with human probiotic features and cholesterol-lowering ability

Santosh Kumar Jana[1,5], Rajarshi Bhattacharya[2,5], Sunanda Mukherjee[3], Samudra Gupta[4], Subhra Prakash Hui[4], Ansuman Chattopadhyay[3], Swadesh Ranjan Biswas[2]✉ & Sukhendu Mandal[1]✉

Research on seed microbiota has gained significant attention due to its role as a primary inoculum that enhances seedling growth, fitness, and productivity. This study explores the characteristics of the plant-probiotic seed-endophyte *Phytobacter* sp. RSE02, which demonstrates distinctive beneficial probiotic features in animal models. We examine the safety and probiotic potential of RSE02 in human cell lines, zebrafish, and mice. Notably, RSE02 can utilize cholesterol as its sole carbon source; however, it does not adhere to the Caco-2 cell line or the zebrafish gut. Importantly, RSE02 is non-toxic across all tested models. We further explore its cholesterol-utilizing ability to determine its efficacy in mitigating hypercholesterolemia and body fat deposits in mice when administered orally. In a high-fat diet mouse model, RSE02 significantly lowered blood cholesterol levels and reduced body weight, peritoneal fat deposits, and liver weight. Additionally, the treatment with RSE02 led to decreased levels of total blood protein, MDA, and GSH in high-fat diet mice. Genomic analysis of RSE02 revealed the absence of virulence or toxin-producing genes while identifying gene clusters responsible for synthesizing key vitamins such as folate, biotin, and vitamin B12. The findings highlight the dual functionality of *Phytobacter* sp. RSE02 in enhancing plant and animal health, challenging traditional notions of probiotics, and offering prospects for innovative solutions in sustainable agriculture and cardiovascular health interventions.

Keywords Seed-endophyte, Probiotic potential, Cholesterol metabolism, Hypercholesterolemia, Gut microbiome

Bacterial endophytes inhabiting the internal tissues of diverse host plants are recognized as the key contributors to plant health and growth[1]. Complex molecular dialogues developed the selective and mutualistic relationships between host plants and endophytes, influencing nutrient acquisition, stress tolerance, and defense mechanisms[2]. Exploration of endophytic community dynamics and their interaction with hosts forms the fundamental groundwork for exploring their potential applications in future agriculture and beyond[3]. Recent research has unveiled various fascinating plant endophytic players from the intricate realm of plant–microbe interactions. Many symbiotic bacteria have gained attention due to their multifaceted roles in promoting plant growth, mitigating stress, and exhibiting biocontrol properties[4]. Our recent investigation characterized five potential seed endophytes of *Oryza sativa* L. (cultivar: Ajinkya 1040), and their effects on enhancing germination, seedling growth, phytohormone production, and controlling fungal and bacterial phytopathogens of rice[5]. Among these, one isolate *Phytobacter* sp. RSE02 was identified as a potential 'plant probiotic' bacterium[5]. The 'plant probiotic' refers to a beneficial microorganism that enhances plant growth, improves nutrient uptake,

[1]Laboratory of Molecular Bacteriology, Department of Microbiology, University of Calcutta, 35, Ballygunge Circular Road, Kolkata 700019, India. [2]Department of Botany, Visva-Bharati, Santiniketan, Birbhum 731235, India. [3]Department of Zoology, Visva-Bharati, Santiniketan, Birbhum 731235, India. [4]SN Pradhan Center for Neuroscience, University of Calcutta, 35, Ballygunge Circular Road, Kolkata 700019, India. [5]Santosh Kumar Jana and Rajarshi Bhattacharya have contributed equally. ✉email: swadesh_s2000@yahoo.co.in; sukhendu1@hotmail.com

and confer resistance against pathogens[6,7], as observed with RSE02's positive impact on seed germination and seedling growth, production of phytohormones, enhancement of mineral cycling, and protection from biotic and abiotic stresses[8–11]. Furthermore, it has been shown that RSE02 can be transmitted from the seeds to the whole plant. The bacterium can be re-inoculated in growing rice seedlings, upon inoculating it in the soil or medium supporting seedling development[5]. Interestingly, the mother plant pre-inoculates beneficial microbes in its seeds and such primary vital inoculum plays an intriguing role in the successful germination, growth, and stress mitigation of its offspring.

Multiple endophytic seed-microbiota have been revealed by scientists through the advancement of the next-generation sequencing facility. The strain RSE02, as present inside the rice seeds, triggers our thoughts about its safety concern for the consumers. Rice often consumed in raw or partially cooked forms in certain traditional preparations, raising valid concerns about the safety of associated microbial strains. Thus, it is a valid enquiry on the level of toxicity or safety of the bacterium has along with its health-benefit attributes.

RSE02 has been identified as a member of the Enterobacteriaceae family, further highlighting its distinctive phylogenetic position within the plant microbiome[1]. The members of the Enterobacteriaceae family consist of both beneficial and harmful species. The close relative of RSE02 is *Phytobacter diazotrophicus*, which is capable of fixing nitrogen. The *Phytobacter* genus has been grouped under the clade *Kosakonia* and later the *Phytobacter* underwent unification with the genus *Metakosakonia*. Many members of the Enterobacteriaceae family such as *Klebsiella*, *Escherichia*, and *Enterobacter* are also established human and animal pathogens[12]. The detailed biochemical and molecular assessment of the strain RSE02 is thus necessary to check if it has any possible toxic or harmful traits.

We evaluated the survival of RSE02 under various stress conditions including different pH levels, salt concentrations, alcohol exposure, gastric juice and pancreatic juice exposures. The adherence of RSE02 with Caco-2 cell line has been tested along with its potential toxicity on these cell lines[13]. RSE02 has been strategically administered to zebrafish to check pathogenicity against this animal model. Further, we have sequenced the whole genome and analysed the genome sequence for any virulence genes as well as for genes that are associated with benefits for the consumers, particularly in relation to probiotic potential[14]. Based on its cholesterol assimilation ability, we administered RSE02 mixed with rice flour to the BALB/c mice which were on a high-fat diet. The total body weight of the mice with the weight of the liver and brain were measured. The levels of the blood cholesterol of the RSE02 treated and untreated mice were also estimated along with their liver function tests[15]. Also, the histochemistry of the brain and liver tissues was envisaged along with measuring total protein, MDA, GSH, and the biological activity of catalase in the gut tissue of the RSE02-fed mice along with the control sets.

The discovery of RSE02 represents a significant advancement in understanding the intricate connections between plant and human microbiomes, revealing a promising area for innovative health applications. The existence of this microbe within the rice seeds suggests a mutualistic relationship with its host, and raising important questions about the potential transfer of beneficial traits from plants to human through rice consumption. Recent studies have unveiled many features of RSE02 as human probiotic bacterium. The major human microbiota primarily residing in the gastrointestinal tract. A potential transfer of plant probiotic bacteria with human probiotic features opens new avenues for understanding the intricate web of microbial interactions in both plants and humans. In this study, we aimed to establish the potentiality of strain RSE02 as a human probiotic bacterium with its ability to lower blood cholesterol levels and develop a unique bridge between agriculture and human health.

Methods

Sample source and bacterial culture

The strain RSE02 (Genbank accession number for 16S rDNA sequence is OM403299) was isolated along with many other endophytic isolates from the seeds of rice (*Oryza sativa* L.) cultivar Ajinkya-1040 collected from a cultivated semi-deep-water paddy field in Malda district, West Bengal (25°16′33″ N 88°00′18″ E)[5]. The rice seed endophyte RSE02 was cultured on Luria–Bertani (LB) agar plates and maintained in the same media for future use[5].

Scanning electron microscopy (SEM) of RSE02

In a previous study, we investigated phenotypic and biochemical features of RSE02[5]. The cellular morphology of RSE02 was determined through scanning electron microscopy (SEM). 1 ml of the overnight grown culture of RSE02 was taken and centrifuged at 6000 rpm for 5 min. Cell pellets were washed twice with PBS and fixed in 0.25% glutaraldehyde present in 100 mM PBS (137 mM NaCl; 2.7 mM KCl; 10 mM Na_2HPO_4; 2 mM KH_2PO_4). 10 µL of the culture was placed on a cover glass, smeared uniformly, dehydrated by different concentrations (v/v) of ethanol (30%, 50%, 70%, 80%, and 90%) and incubated for 10 min followed by treating with 100% ethanol and incubated for 1 h. Then the sample was observed under a scanning electron microscope (ZEISS EVO 18 Special Edition).

Labelling of RSE02 genome with RFP

In order to track the endophytic RSE02 inside zebrafish gut and to examine its ability to adhere with cell line, the red fluorescence protein (RFP) coding gene-cassette containing plasmid (pUC18T-mini-*Tn*7T-Gm-dsRedExpress) was incorporated into the RSE02 strain through tetra-parental conjugation strategy described by Patra et al. 2024[16]. In brief, the log phase suspension of recipient cells, RSE02 (gen^R, tmp^S), donor cells having a plasmid with RFP coding gene and mini-*Tn*7, helper-1 cells (*E. coli* DH5 ∝ + pTNS2; amp^R), and helper-2 cells (*E. coli* HB101 + pRK2013; kan^R) were cultured in Luria–Bertani (LB) medium. The cultures were centrifuged at 6000 rpm for 5 min, and cell pellets were washed with fresh LB; co-cultured on a filter membrane at a ratio of 2:4:1:1.5 to facilitate mini-*Tn*7-mediated transfer of the RFP coding gene into the genome of the recipient cell.

All cell types, i.e., recipient, donor, helper 1 and helper 2 were suspended in LB broth to 0.6 OD ($A_{600\ nm}$) at a ratio of 2:4:1:1.5. Then the mixture was centrifuged and washed with fresh LB medium and incubated at 28 °C for 1 h. After incubation, cell suspensions were added on a filter paper (0.22 µm) which was carefully placed on a mating (LB agar) plate and incubated at 28 °C for 24 h. Then the filter paper was suspended in 0.9% NaCl and slightly vortexed to remove the cells. Finally, dilutions of the suspended cells were used for the selection of RSE02 transconjugants by growing on an LB medium containing a mixture of two antibiotics (gentamycin 30 µg/mL and trimethoprim 30 µg/mL). The RSE02 transconjugant was confirmed using fluorescence microscopy.

Whole genome sequencing

The whole-genome-based taxonomy analysis of strain RSE02 (WGS accession number PRJNA1127180) was carried out by type strain genome server (TYGS) (at https://tygs.dsmz. De)[17]. The phylogenomic tree was constructed using FastME[18] from the genome blast distance phylogeny (GBDP). For this, GBDP and inter-genomic distances determined using the 'trimming' algorithm and distance formula d5 was used for all pair-wise genome comparisons. The inference of branch supports was derived using 100 pseudo-bootstrap duplicates[17].

The average nucleotide identity (ANI) values, such as ANI-Blast (ANIb) and ANI-MUMmer (ANIm) and Tetra algorithms were used to calculate strains by using JSpecies WS software[19,20]. The genome-to-genome distance calculator (GGDC 3.0; http://ggdc.dsmz.de) was used to calculate digital DNA–DNA hybridization (dDDH) values between the genome of both strains and the closely related species, using the recommended BLAST + method [21–23]. The dDDH results were based on recommended formula 2 (identities/HSP length), which is not affected by genome length and thus can serve as a robust indicator for incomplete draft genomes.

Genome analysis

To classify the functional features of the genes from the draft genome sequence, the coding sequences of the RSE02 strain were compared against the KEGG and COG databases[24]. The genes associated with probiotic features were identified by comprehensive genome annotation using tools such as eggNOG, InterPro, KEGG mapper, pannzer2, and RAST. The whole genome sequence of RSE02 was analyzed using Proksee (https://proksee.ca)[25], which generated a circular map with features annotated from the outermost to the innermost circle. BLAST alignment with the reference genome *P. diazotrophicus* (GCA_004346725.1), Prokka annotated features in the positive and negative strand, contigs of the RSE02 assembly, GC content, GC skew, genome size, gene distribution and statistical result of functional genes presents in the RSE02 genome subsystem were analyzed. Furthermore, vitamin (Biotin, Folate, Riboflavin, and related vitamins) producing gene clusters associated with probiotic features were identified by comprehensive genome annotation using Proksee and RAST.

Characterization of the probiotic potentials of RSE02

Comparative stress tolerance of the probiotic isolates To determine the various stress tolerances, that are considered essential criteria for establishing a microorganism as a probiotic, RSE02 was grown in 1% glucose containing MS medium (8.0 g of K_2HPO_4, 1 g of KH_2PO_4, 0.5 g of $(NH_4)_2SO_4$, 0.2 g of $MgSO_4.7H_2O$, 1 g of NaCl, 0.1 g of $Ca(NO_3)_2$, 20 mg of $CaCl_2.2H_2O$, 20 mg of $FeSO_4.7H_2O$, 0.5 mg of $Na_2MoO_4.H_2O$, and 0.5 mg of $MnSO_4$ per litre of deionized water) supplemented with varying concentration of bile (0.3%, 0.5%, 1% w/v), NaCl (4%, 6% w/v), varying pH (4 to 12), pancreatin (0.5% w/v), phenol (0.5% v/v), varying concentration of ethanol (10%, 15%, 20% v/v), pancreatin (0.5% w/v) and gastric juice (pH 3)[26,27]. The culture was inoculated with 2% overnight grown seed-inoculum and incubated in shaking condition (180 rpm) at 37 °C for 24 h. Control cultures were grown in 1% glucose containing MS medium. Growth of RSE02 was determined by measuring optical density at 600 nm using a spectrophotometer and counting the CFUs. Therefore, simulated gastric juice was prepared by using 3 g/L pepsin, 7 mM KCL, 45 mM $NaHCO_3$, and 125 mM NaCl, adjusting the pH at 3 and 7 (control) with appropriate amount of 1 M HCL and 1 M NaOH, respectively[28]. The simulated gastric juice (pH 3) was inoculated with overnight grown RSE02 culture (2%) and incubated in shaking condition (180 rpm) at 37 °C for 24 h.

Carbon utilization assay and sugar fermentation assay

The ability of the isolate to utilize different carbon sources were assessed by using HiCarbo Kit from Himedia, India. The experiment was performed according to the manufacturer's protocol. Growth and acid production of RSE02 was monitored by evaluating carbon source utilization and fermentation profiles.

Cell surface hydrophobicity

Cell surface hydrophobicity of RSE02 was assessed to evaluate its adherence potential to the gut epithelium. Overnight-grown cultures were centrifuged at 5000 rpm for 10 min. The cell pellet was washed twice with PBS, re-suspended in PBS buffer, vortexed, and adjusted to an absorbance of 0.7 −0.9 (A_0) at 600 nm. 5 mL of the suspension were mixed with an equal volume of hydrocarbons (chloroform, ethyl acetate and xylene) and incubated at 37 °C for 24 h to allow phase separation. 1 mL from the aqueous phase was collected, and absorbance was measured at 600 nm (A_1). The percentage of hydrophobicity was calculated using the following formula:

$$\text{Hydrophobicity } (\%) = (1 - \text{A1/A}) \times 100$$

Auto aggregation

Auto-aggregation was evaluated following the method described by Manvelyan et al. (2023)[29]. RSE02 cells were harvested from overnight cultures by centrifugation (5000 rpm, 10 min), washed with PBS, and resuspended to an absorbance of 0.5 at 600 nm (A_{ini}). The suspension was incubated in tubes at 37 °C for 2 and 24 h. After

incubation, 1 mL from the upper phase was removed carefully to measure absorbance at 600 nm (A_{fin}). Cell auto-aggregation was determined by a decrease in absorbance and measured by using the following formula:

$$\text{Percentage of auto} - \text{aggregation} = (A_{ini} - A_{fin}) / A_{ini} \times 100.$$

Coaggregation

For co-aggregation, RSE02 was prepared as described in above paragraph. Equal volumes of RSE02 and either probiotic or pathogenic bacterial suspensions were mixed and incubated at 37 °C without agitation. The absorbance (at 600 nm) of the mixtures were monitored at 0 h and 24 h; along with the absorbance for the bacterial suspensions alone. Co-aggregation was calculated as follows:

$$\{[(A_{PAT} + A_{PRO})/2 - A_{mx}] / (A_{PAT} + A_{PRO})/2\} \times 100,$$

where A_{pat} and A_{pro} represent in control tubes and A_{mx} represents the absorbance of the mixed bacterial suspension at 24 h.

Bile salt hydrolase activity

The bile salt hydrolase (BSH) activity was determined using a direct plate assay[30]. RSE02 was spotted on MS agar plates supplemented with 1% glucose, with 0.5% (w/v) $CaCl_2$, and 0.3% bile salt. The plates were incubated at 37 °C for 72 h, while MS plates without these supplements were used as control. The presence of precipitated bile salt around colonies or the formation of colonies with a silvery shine was considered as BSH activity.

Cholesterol lowering activity

RSE02's ability to assimilate cholesterol was assessed in MS medium supplemented with 100 µg/mL water-soluble cholesterol. The medium was inoculated with 2% overnight culture and incubated at 30 °C with shaking (180 rpm). Bacterial growth was monitored spectrophotometrically at 600 nm at 0, 6, 12, 18, 24 and 48 h. The uninoculated medium served as control. Cell-free supernatant were obtained by centrifugation (6000 rpm for 15 min at 4 °C). To 500 µL of supernatant, 500 µL of 33% (w/v) KOH (and 1 mL absolute ethanol were added. The mixture was vortexed for 1 min and incubated at 37 °C for 15 min. Subsequently, 1.5 mL n-hexane and 1 mL distilled water were added and mixed thoroughly. After phase separation (15 min), 500 µL of upper hexane layer was transferred to a glass-tube and evaporated in a 65 °C water bath till dryness. The dried sample was dissolved in 1 mL of $FeCl_3$ (0.5 mg/mL) followed by the addition of 250 µL concentrated H_2SO_4. After 30 min incubation in the dark, absorbance was measured at 570 nm[31]. The cholesterol assimilation ability (µg/mL) was calculated as follows:

$$\text{Cholesterol assimilation} = 100 - (B/C) \times 100,$$

where B is absorbance of the test sample and C is that of the control.

Preparation of bacterial cell lysate

RSE02 was grown in LB medium for overnight at 30 °C in shaking condition (180 rpm) to study their toxicity effect. 1 ml (1×10^9 CFU/mL) of the RSE02 culture was taken and ultra sonicated at 65 Hz. The cell suspension was then centrifuged at 13,000 rpm for 10 min and supernatant was collected and used for further study.

Cell line and cell culture

Caco-2 cells were maintained in Dulbecco's Modified Eagle's medium (DMEM, Sigma Chemical Co., St. Louis, MO) supplemented with 10% fetal bovine serum (Invitrogen) and 100 µg/mL penicillin and streptomycin. Cells were cultured in 75 cm^2 filter–capped flasks at 37 °C in 5% CO_2 incubator. When cells were reached the log phase, the cell density was adjusted to 1.0×10^2 per well using fresh DMEM. This culture was used to inoculate with 1000 µL (1.0×10^4 cells) of cell suspension in each glass bottom dish. After adhesion the medium was removed, cells were washed three times with PBS (pH 7.0), and processed as required.

MTT assay

Cytotoxicity of the RSE02 lysate was determined using MTT assay as per Mosmann, 1983[32]. Approximately 7500 Caco-2 cells in 100 µL were seeded into each well of a 96-well plate and incubated at 37 ℃ for 24 h in a CO_2 incubator. 10, 20 and 30 µL lysate from 1×10^9 CFU/mL RSE02 suspension were applied to each well of the microplate in triplicate. 20 µL of MTT reagent was added to each well and incubated for an additional 3 h after the initial 24 h of incubation. Once purple formazan crystals formed, 150 µL of MTT solvent was added, and absorbance was measured at 590 nm using a VARIOSKAN LUX plate reader (Thermo Scientific). Wells lacking cells served as blanks; wells without lysate served as positive controls.

Cell adhesion assay

To study the adhesion ability of RSE02 to the Caco-2 cell line, both were co-incubated, and adherence was confirmed by microscopic visualization as described by Palaniyandi et al. 2020[33]. Briefly, 35 mm glass bottom culture plates were seeded with 1×10^5 cells in 1000 µL of DMEM medium and incubated for 12 h at 37 ℃ in a 5% CO_2 incubator. The cells were incubated with 1×10^6 CFU/mL RFP-labelled RSE02 bacterial cell for 2 h at 37 ℃ in a 5% CO_2 incubator after 500 µL PBS (pH 7.4) wash and cells without RFP-labelled RSE02 bacterial cells were used as control. After successful incubation, the plate was washed again with 500 µL PBS to remove any free bacteria that could not attached to the Caco-2 cell line. Both the animal and bacterial cells were stained with

DAPI (1 µg/mL) for 10 min. Then cells were washed carefully several times with 1X PBS (pH 7.4) to remove the untied stain properly. Finally, cell imaging and bacterial adhesion ability were done under Phase contrast, DAPI and TRITC filter under 40X magnification in the Olympus IX73 cellSens standard fluorescence microscope.

Zebrafish maintenance

Adult zebrafish of the AB strain aged 3–6 months were used in this study. Fish were maintained in custom-built aquaria tanks at a density of approximately 5 fish per litre and at a water temperature of 28 ℃. All zebrafish husbandry and experiments were conducted in accordance with institutional and national animal ethics guidelines and were approved by the Committee for the Purpose of Control and Supervision of Experiments on Animals (CPCSEA). All experiments used control and experimental groups comprising fish of similar size and balanced sex distribution.

Production of conventionally raised and germ-free (GF) zebrafish

Newly hatched eggs were collected immediately after hatching and transferred to standard zebrafish E3 culture medium (5 mM NaCl, 0.17 mM KCl, 0.33 mM $CaCl_2$, 0.33 mM $MgSO_4$). For the conventionally raised zebrafish, embryos were maintained in unsterilized E3 medium supplemented with 0.05 mg/mL sea salt. Larvae were reared under controlled conditions at 28 °C with a 14 h light ad 10 h dark photoperiod. The culture medium was replenished daily to maintain optimal physicochemical conditions and reduce microbial accumulation.

Germ-free (GF) zebrafish embryos were generated following established protocols[34], with some modifications. Briefly, fertilized embryos obtained from adult zebrafish were washed three times with sterile water (3 min per wash at room temperature), then incubated at 28 °C for 6 h in antibiotic-supplemented E3 medium. This medium contained 0.05 mg/mL sea salt, 100 µg/mL ampicillin, 5 µg/mL kanamycin, and 250 ng/mL amphotericin B (all from Sigma, St. Louis, USA). Subsequently, the embryos were immersed in a 0.05% polyvinylpyrrolidone (Sigma, St. Louis, US) solution for 30 s, followed by three subsequent washes using sterile E3 medium. Embryos were then treated with 0.002% sodium hypochlorite solution (SRL, Mumbai, India) for 10 min to further eliminate potential microbial contaminants, followed by three additional rinses with sterile E3 medium. Embryos were transferred to sterile 6-well culture plates at a density of 5 embryos per 10 mL of sterile E3 medium and maintained at 28 °C under the same photoperiod conditions as conventionally raised fish. To prevent the accumulation of waste and ensure adequate dissolved oxygen levels, 50% of the E3 media in each well was replaced with fresh sterile medium daily, as previously recommended[35]. To conform germ-free status, aliquots of the culture medium from each well were collected daily and plated on Luria–Bertani (LB) agar plates. These were incubated under both aerobic and anaerobic conditions at 38 °C for 48 h to detect any microbial growth[36].

Production of GF mono-associated zebrafish by RSE02 exposure

To prepare bacterial suspensions, RSE02 was cultured, then centrifuged at 7500 rpm for 10 min to pellet the cells. The supernatant was discarded, and the bacterial pellet was washed three times with sterile distilled water to remove residual medium. The washed pellet was resuspended in sterile E3 medium and introduced into the medium used for GF zebrafish. GF zebrafish larvae were randomly divided into two experimental groups: GF control and GF mono-associated. The GF mono-associated group was subjected to RSE02 at final concentrations of 1×10^9, 2×10^9, and 4×10^9 CFU/mL for 72 h at 28 °C. After the exposure period larvae from each group were washed five times with sterile E3 medium to eliminate any surface-adhering bacteria. Subsequently, they were subjected to fluorescent microscopy using an Olympus BX53F2 microscope (Olympus, Tokyo, Japan) to ascertain the presence of the bacterial strain within the gastrointestinal tract.

The zebrafish larvae were homogenized using a micropestle in autoclaved 1 × PBS to release bacteria within the body. Serial dilutions of the recovered suspensions were then plated onto Luria–Bertani (LB) agar plates supplemented with kanamycin to facilitate the detection of RSE02 expressing red fluorescent protein (RFP).

Bacterial exposure on adult zebrafish

To evaluate the effects of RSE02 exposure on adult zebrafish, bacterial cultures were prepared as described previously[37], with minor modifications. Briefly, RSE02 was grown in TSB at 25 °C with shaking at 140 rpm for 24 h. The culture was centrifuged at 6000 rpm for 15 min at room temperature, and the pellet was resuspended in sterile PBS. Before the assay, the non-lethal dose (not causing mortality) was determined by exposing zebrafish to three bacterial concentrations (1×10^9 CFU/mL, 1×10^{10} CFU/mL, and 2×10^{10} CFU/mL) according to the in vitro dose.

A total of 10 adult zebrafish were taken in a tank containing 10 L system water and exposed by immersion to RSE02 (1×10^{10} CFU/mL) for first 5 days with normal feeding and last 2 days without any bacterial exposure. Fishes exposed to 1X PBS and system water were considered as control groups.

Tissue collection and fluorescence microscopic analysis of zebrafish gut sections

After the exposure period, adult zebrafish gut tissues were dissected and fixed in 4% paraformaldehyde (Sigma) for 8 h or overnight at 4 ℃. Fixed tissues from both control and experimental groups were embedded in O.C.T compound (Leica) and cryosectioned at 10 µm thickness. Tissue sections were stained with DAPI for 15 min at room temperature. After washing in PBS, the sections were mounted with Gelvatol mounting medium (Vector Labs, Burlingame, CA) and photographed by using OLYMPUS BX53F2 microscope (Olympus, Tokyo, Japan).

Gut content analysis

Intestinal tracts from all experimental and control zebrafish were dissected under sterile conditions. The content were gently expelled onto clean glass slides to prepare smears, which were air dried for 1–2 h and fixed with methanol for subsequent microscopic analysis.

Animal maintenance and grouping

30 BALB/c mice (*Mus musculus*), evenly distributed between male and female (n = 15 each) were u procured from a certified breeding facility. The animals were maintained in the institutional animal care facility under controlled environmental conditions: 12 h light/dark cycle, 22 ± 2 °C temperature, and 50 ± 10% relative humidity. Mice were housed in polypropylene cages (5 mice in each cage) with stainless steel grill tops and autoclaved rice husk bedding. Experimental procedures followed the guidelines of the Institutional Animal Care and Use Committee (Approval Number: IAEC/VB/2022-IV/06). Three different experimental sets were formed: (a) Placebo Control (PC) (n = 10): mice received a standard diet and placebo treatment, (b) High Fat Diet (HFD) (n = 10): mice received a high-fat diet (c) High Fat Diet + RSE02 treatment (HFD + RSE02) (n = 10): mice received a high-fat diet followed by RSE02 treatment.

Dietary regimen

All mice, except those in the placebo group, were fed a high-fat diet consisting of 60% fat, 20% protein, and 20% carbohydrates for 30 days. The control group received a standard chow diet. RSE02 was cultured in nutrient broth at 37 °C for 18 h, centrifuged at 5000 rpm for 10 min, and the pellet was resuspended in sterile saline to a final concentration of 10^8 CFU/mL. After the initial dietary intervention, the HFD + RSE02 group received 200 µL of the bacterial suspension mixed with rice flour daily for 15 days. The PC and HFD groups received an equivalent volume of saline mixed with rice flour.

Blood sample collection and lipid profiling

On the 15th day of probiotic treatment, blood samples were collected from three randomly selected mice from each group via retro-orbital puncture under mild anesthesia. Serum was collected from the blood samples after these got clotted. The samples were then centrifuged at 3000 rpm for 10 min to separate the serum. Total cholesterol (TC), triglycerides (TG), high-density lipoprotein cholesterol (HDL-C), and low-density lipoprotein cholesterol (LDL-C), present in the serum samples were determined using an automated analyzer (Beckman Coulter, USA).

Biochemical analysis

This experiment was conducted following the protocol of Beutler, 1963[38]. In short, liver tissues were collected using sterile forceps and scissors from freshly dissected control and treated mice. The tissues were then blanched with phosphate buffer saline (PBS) and a 10% homogenate was prepared. It was further added with an equal volume of 20% TCA solution, keeping it in ice. The mixture was centrifuged at 6000 rpm for 5 min. Next, 0.3 M di-sodium hydrogen phosphate buffer and 0.1 mg/mL DTNB solution in 3:1 ratio, was added with 1 ml of supernatant collected after centrifugation. After 5 min, the value of optical density (OD) of each individual sample was taken at a wavelength of 412 nm. The amount of GSH contents were denoted as micromolar (µM) reduced glutathione per milligram of protein.

Catalase (CAT) activity was assessed following Aebi, 1984[39]. Liver tissues were homogenized in PBS and centrifuged at 10,000 rpm for 20 min at 4 °C. The assay mixture contained 980 µL of catalase assay buffer (50 mM Tris–HCL of pH 8.0, 9 mM of H_2O_2 and 0.25 mM of EDTA) and 20 µL of supernatant. Finally, the decline of optical density value per minute of the reaction mixture of each sample was recorded at 240 nm for 1 min. Results were represented in terms of unit (U) per milligram (mg) of total protein.

Lipid peroxidation was quantified via thiobarbituric acid reactive substances (TBARS) assay as described by Buege & Aust, 1978[40]. Liver tissues were homogenized in PBS and centrifuged at 3000 × g for 15 min. The supernatant (1 mL) was mixed with reaction mixture (thiobarbituric acid + trichloroacetic acid + hydrochloric acid) in 1:2 (v/v) ratio, boiled for 15 min, cooled and centrifuged at 1000 × g for 10 min. OD was measured at 535 nm. Malondialdehyde (MDA) levels were calculated using an extinction coefficient of 1.56×10^5/M/cm and expressed as nM MDA/mg protein.

Histological analysis

Zebrafish were euthanized by cold shock, and the gut tissues were dissected under sterile conditions. Mice were anesthetized using ketamine and disinfected with 70% ethanol prior to sacrifice. The ventral side of the mice was opened up and liver tissues were dissected out using autoclaved scissors for further experiments. Following sacrifice, liver tissues from control and all the treated mice were immediately immersed in adequate amount of Bouin's fixative for proper fixation. The tissues were dehydrated through graded alcohol and fixed in paraffin wax, and 5 µm thin tissue pieces were made using microtome. Hematoxilin and eosin staining was done for proper visualization of internal structures with an upright light microscopy (Leica DM3000, Leica Microsystems GmbH, Wetzlar, Germany).

Determination of serum SGPT and SGOT

Levels of serum SGPT and SGOT were analyzed using commercial kit of Nanjing Jiancheng Bioengineering Institute, Nanjing, China; following manufacturer's protocol.

Ethical considerations

All experimental protocols involving mice were conducted in accordance with the ethical standards approved by the IACUC of Visva-Bharati University (Approval Number: IAEC/VB/2022-IV/06).

Statistical analysis

Statistical analysis was performed using GraphPad Prism (version 8.0). Data were expressed as mean ± standard error of the mean (SEM). Differences between groups were analyzed using one-way ANOVA followed by Tukey's post hoc test and Dunnett's multiple comparisons test. A p value of < 0.05 was considered statistically significant. Survival curves were analysed using the Kaplan–Meier method (GraphPad Prism version 6.00, GraphPad Software, La Jolla California USA). All experiments were done in triplicate for a total of 10 fish per condition.

Results

Phytobacter as a rice seed endophyte with probiotic potential

Our study identified *Phytobacter* sp. RSE02 as an endophytic rod-shaped bacterium. Whole genome sequence-based phylogenomic analysis clustered RSE02 closely with other members of the *Phytobacter* genus, with *P. diazotrophicus* being the nearest relative (Fig. 1). *Phytobacter* sp. RSE02 resides within rice seeds as an endophyte and showed plant probiotic potentiality by production of phytohormones (IAA & GA), siderophore and HCN[5].

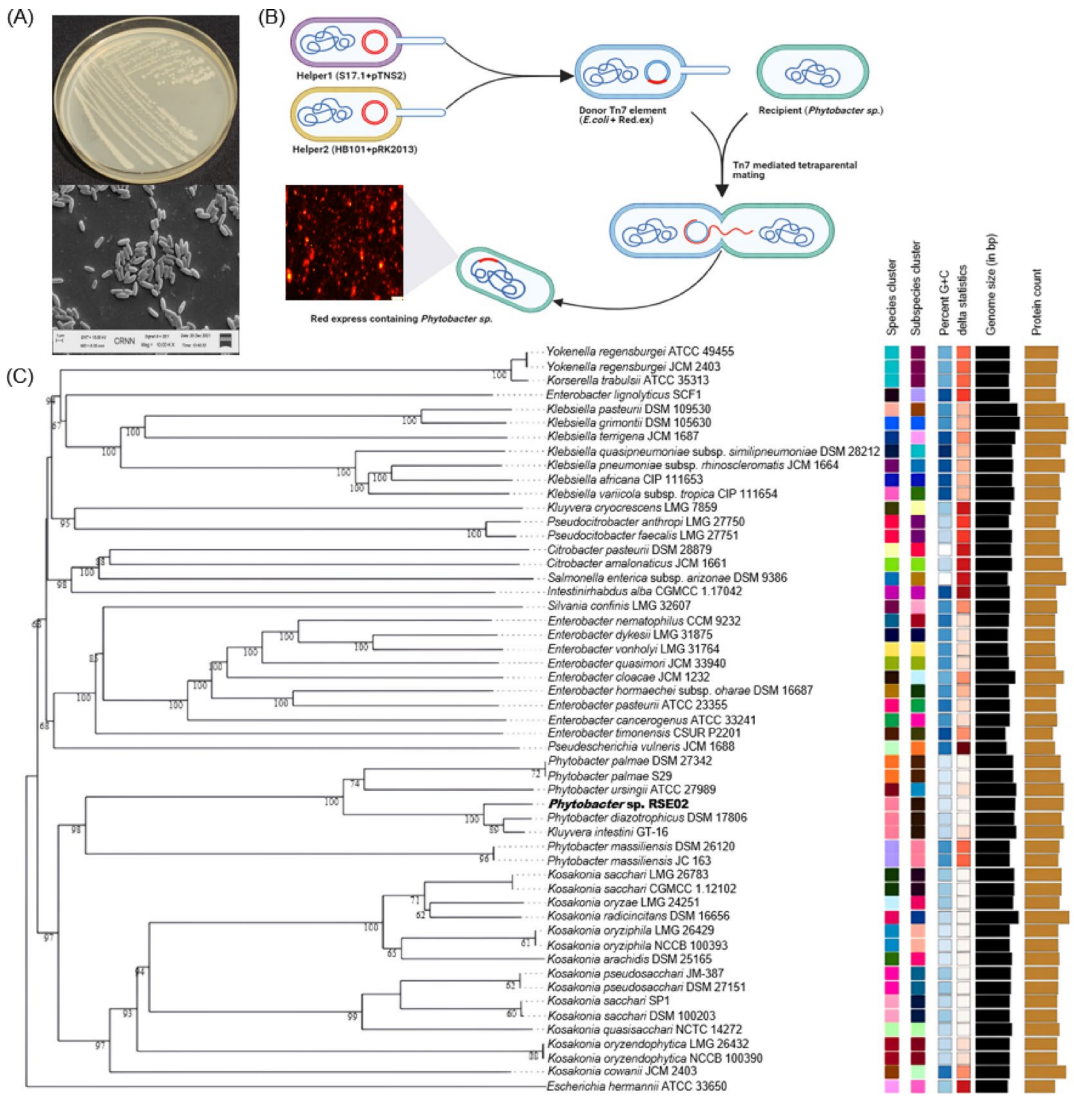

Fig. 1. (**A**) Colony morphology and SEM image of RSE02 probiotic strain. (**B**) Tn7 mediated RFP- gene transfer mechanism to fluorescence labelle RSE02 strain. (**C**) Phylogenomic tree based on whole genome sequences of the representative RSE02 strains in the TYGS tree inferred with FastME 2.1.6.1 [17,24] from Genome BLAST Distance Phylogeny approach (GBDP); distances calculated from genome sequences. The branch lengths are scaled in terms of GBDP distance formula d5. The numbers above branches are GBDP pseudo-bootstrap support values > 60% from 100 replications, with an average branch support of 93.7%. The tree was rooted at the midpoint[20].

To track RSE02 inside the host, we have successfully labelled it by tagging its genome with RFP-gene cassette (Fig. 1B). This will help in further investigation of the multifaceted roles of *Phytobacter* sp. RSE02 in both agricultural and human health contexts. Biochemical analyses indicated that RSE02 exhibited the salient features of standard probiotic bacteria, emphasizing its suitability for further investigation.

RSE02 survives in gastrointestinal mimicked environment

Ethanol is commonly present in fermented foods and beverages, as well as in certain probiotic formulations and industrial process settings; therefore, tolerance to ethanol serves as a critical parameter in evaluating a strain's resilience and functional stability. The ability of a probiotic candidate to withstand chemical stress indicates its robustness, adaptability, and suitability for incorporation into alcohol-containing functional foods and nutraceutical products. Moreover, ethanol tolerance can reflect a strain's capacity to endure the metabolic by-products generated during microbial fermentation, further supporting its potential efficacy and viability as a probiotic agent. Thus, tolerance to elevated NaCl is a desirable trait for probiotic strains intended for oral consumption, as it enhances their survival and functional persistence during gastrointestinal transit. Additionally, NaCl tolerance is critical for maintaining cell viability during manufacturing, storage, and incorporation of high-salt fermented foods such as kimchi, sauerkraut, and brined vegetables. In general, phenols accumulate, particularly in the distal colon, where microbial fermentation predominates, and can exert deleterious effects on both host epithelial cells and commensal or ingested bacterial strains due to their membrane-disruptive and protein-denaturing properties.

RSE02 showed substantial tolerance when grown in the presence of 10% alcohol, 4% NaCl and 0.5% phenol (Fig. 2A). It also exhibits considerable hydrophobicity and an auto-aggregation phenotype during growth (Fig. 2B). RSE02 demonstrated robust survival in a simulated gastrointestinal environment (Fig. 2A), suggesting its ability to withstand the harsh acidic environment of the stomach of the host. Although the optimum pH for its growth has been observed to be neutral, it can survived in the pH range of 5–12 (Fig. 2C). This resilience is a crucial trait for probiotic bacteria aiming to reach and exert their effects in the intestine. Furthermore, the strain tolerated 0.3% bile salt and showed growth enhancement when the medium was fortified with 0.5% pancreatin. The ability of RSE02 to survive in a gastrointestinal (GI) mimicked environment suggests its potential application not only in agriculture but also in human health[41]. The resilience of RSE02 opens avenues for exploring its dual functionality as a 'plant probiotic' with implications for human well-being.

The observed alcohol, NaCl, and phenol tolerances of *Phytobacter* sp. RSE02 supports its viability and potential probiotic function in the chemically complex and metabolically active environment of the human intestine.

Probiotic features of RSE02 and its nutraceutical and therapeutic potential

RSE02 displayed cholesterol utilization features (Fig. 3A), indicating its possible future application in nutraceutical and therapeutic fields. This strain also exhibited bile salt hydrolase activity (Fig. 3B) which has broader health-promoting and cholesterol-lowering potential. It is known that the BSH deconjugates bile salts and reduce their reabsorption. Thus, the body uses more cholesterol to synthesize new bile acids, thereby lowering the serum cholesterol levels. These features highlight the potential of RSE02 as a multifunctional agent with applications in agriculture and the development of therapeutic agents for human use. RSE02 extends its probiotic prowess beyond traditional functions by exhibiting nutraceutical and therapeutic potentials[42].

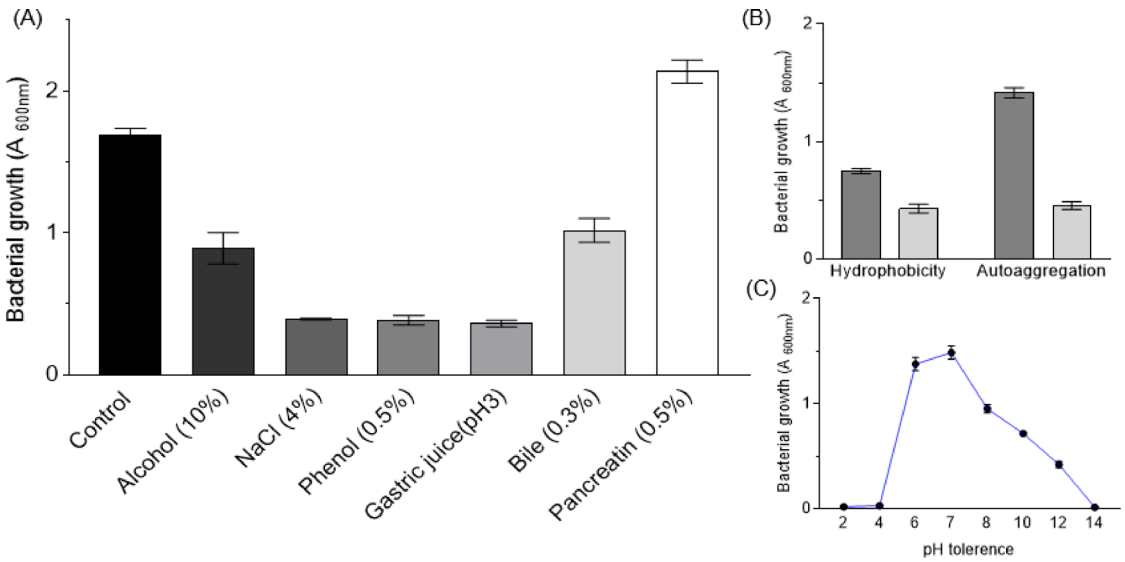

Fig. 2. Probiotic potential of RSE02 bacterial endophyte. (**A**) Biochemical analysis of RSE02 bacteria. (**B**) Hydrophobicity and Auto-aggregation of strain RSE02 (dark grey bar: 0 h; grey bar: after 24 h). (**C**) pH tolerance (2 to 14) of strain RSE02.

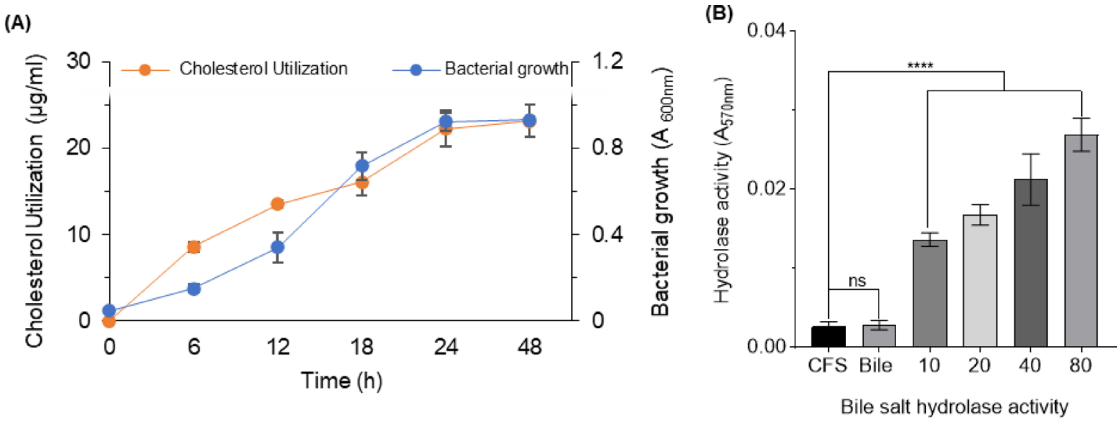

Fig. 3. Cholesterol utilization and Bile salt hydrolase activity test. (**A**) In-vitro cholesterol utilization by the RSE02 strain in different time (0, 6, 12, 18, 24 and 48 h) interval, where initial cholesterol concentration was 100 µg/mL in minimal medium. (**B**) Bile salt hydrolase (BSH) activity of the RSE02 strain was assessed by the qualitative direct plate assay.

Genome sequence indicates RSE02 as a safe probiotic bacterium

Whole-genome sequence analysis revealed a 6 Mbps genome size consisting of the imprints of multiple probiotic features (Fig. 4). A comprehensive understanding of the probiotic potential of RSE02 requires a detailed analysis of its genomic landscape. Genome sequence analysis indicated the absence of virulence factors and the presence of genes associated with coding compounds with beneficial functions, such as biotin, folate, and riboflavin establishing RSE02 as a safe probiotic bacterium (Fig. 4)[43]. Experimental studies on animal models and clinical investigations in humans have demonstrated that biotin supplementation leads to significant reductions in serum triglyceride and low-density lipoprotein (LDL) cholesterol levels, alongside increases in high-density lipoprotein (HDL) levels. The cardioprotective role of folate-producing probiotics has been substantiated in previous in vivo studies, further supporting the hypothesis that endogenous folate synthesis by *Phytobacter* sp. RSE02 contributes to the observed hypocholesterolemic phenotype. Riboflavin (vitamin B2) plays a fundamental role in cellular energy metabolism and lipid catabolism as a precursor of flavin mononucleotide (FMN) and flavin adenine dinucleotide (FAD).

Genome sequence analysis and comparative genomics

Once we observed the possibility of application of RSE02 as a plant and animal probiotic was observed, we attempted to determine its taxonomic status. To segregate RSE02 from closely related known strains, several in silico methods (dDDH, ANIm, ANIb, Tetra, and difference of G + C) were used. The dDDH values between RSE02 and its four closest strains *Phytobacter diazotrophicus* DSM 17806, *Kluyvera intestine* GT-16, *P. ursingii* ATCC 27989, and *P. palmae* S29 were 88.2, 83.7, 74.7, and 80.4, respectively (Table 1). The ANIm, ANIb and Tetra values between RSE02 and *P. diazotrophicus* and *K. intestini* were above the cut-off level (> 95%, > 95% and > 0.999) and between *P. ursingii* and *P. palmae* were below the cut-off level (< 95%, < 95% and < 0.999) recommended as the average nucleotide identity (ANI) criterion for closely related species[18] (Table 1). The differences in G + C content between RSE02 and the four closely related strains were 0.24, 0.21, 0.11, and 0.23, respectively (Table 1). The TYGS-based phylogenomic analysis revealed that the RSE02 strain showed the highest sequence similarity to *Phytobacter diazotrophicus* DSM 17806 (Fig. 1C).

RSE02 does not adhere with caco-2 cell line

Unlike many established probiotics, RSE02 did not show visible adherence properties to the Caco-2 cell line under the tested experimental conditions (Fig. 5AI–IV). This characteristic of RSE02 challenges conventional notions on probiotic[44]. This distinctive interaction pattern raises intriguing questions about the mechanisms through which RSE02 influences host health, warranting further investigation.

RSE02 is non-toxic to human cell lines and zebrafish

To assess safety, RSE02 was tested for toxicity against adult zebrafish and human cell lines (Fig. 5B, C). The results indicated no cytotoxic effects, affirming its safety profile and potential therapeutic applications.

Safety assessments are paramount when considering the application of probiotics to human health. The non-toxicity of RSE02 to human cell lines and zebrafish provides reassuring evidence of its safety[45]. This safety validation positions RSE02 as a candidate for further exploration of therapeutic interventions, reinforcing its potential applications beyond agriculture.

RSE02 passes gastric environment and is present in live form in the intestine

In an in vitro model simulating gastric conditions, RSE02 exhibited survival and viability. Moreover, live bacteria were recovered from the intestines of RSE02-fed adult zebrafish (Fig. 5D & eI–IV), signifying its ability to transit through the stomach of the fish and establish its presence in the intestines. The successful passage through

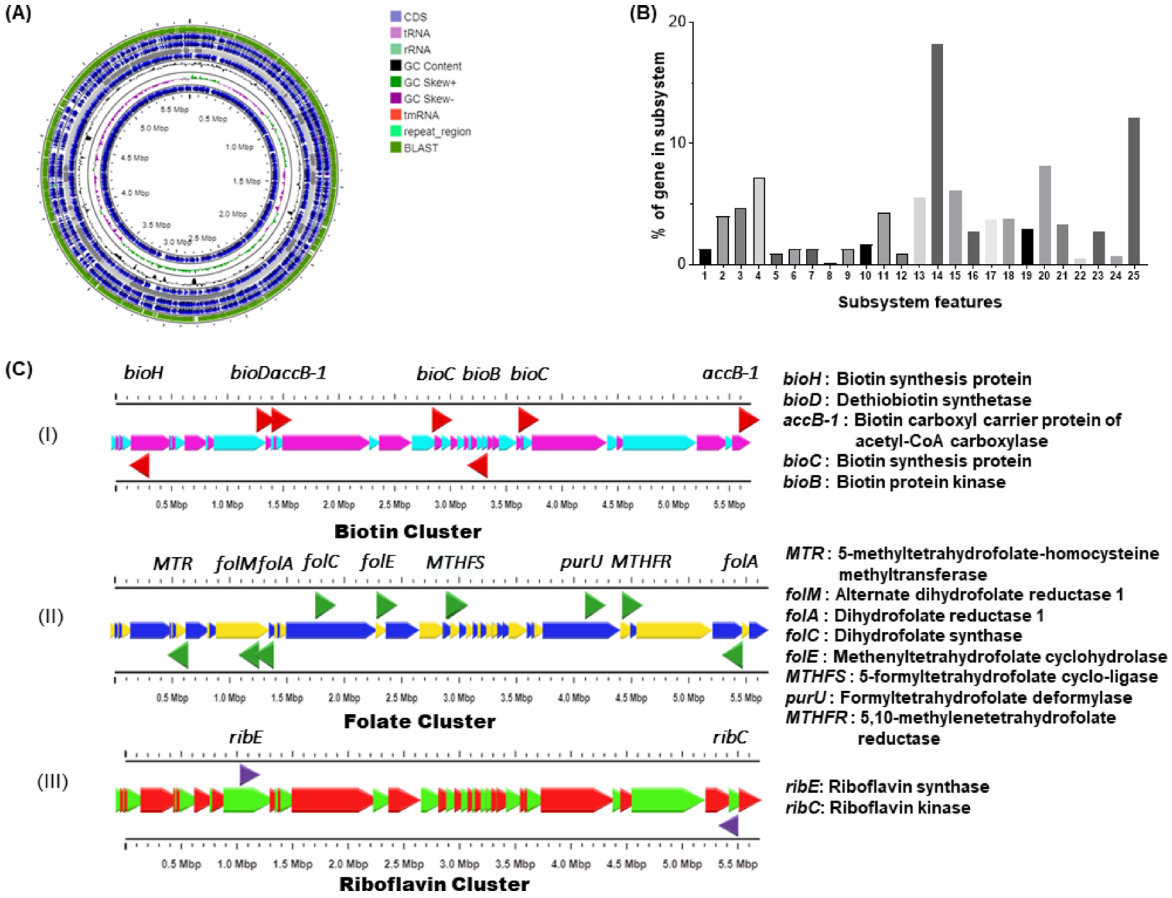

Fig. 4. Whole genome sequence analysis of the strain RSE02. (**A**) represents the circular genome map showing arrangement of CDs, RNAs etc. (**B**) represents abundance of major gene-subsystems (Where:1–25 represents N_2 metabolism; respiration; stress response; protein metabolism; cell division and cell cycle; sulfur metabolism; phages, prophages, transposable elements, plasmid; secondary metabolism; iron acquisition and metabolism; membrane transport; phosphorus metabolism; RNA metabolism; carbohydrates; cell wall and capsule; DNA metabolism; regulation and cell signalling; fatty acids, lipids and isoprenoids; motility and chemotaxis; cofactor, vitamins, prosthetic groups, pigments; nucleosides and nucleotides; metabolism of aromatic compounds; virulence, disease and defense; potassium metabolism; amino acids and derivatives; dormancy and sporulation respectively. (**C**) represents presence of beneficial genes and gene clusters in respect of the probiotic potentials, and (**D**) shows representative biosynthesizing gene clusters of biotin, vitamin B12, folate and bacteriocin[24].

Isolate name	Closest ancestors	dDDH[1] (%)	ANI[2] (%)		Tetra	Difference G + C
			ANIm	ANIb		
RSE02	*Phytobacter diazotrophicus* DSM 17806	88.2	97.97	97.69	0.99974	0.24
	Kluyvera intestini GT-16	83.7	98.00	97.62	0.9997	0.21
	Phytobacter ursingii ATCC 27989	74.7	91.86	91.25	0.9979	0.11
	Phytobacter palmae S29	80.4	91.88	91.25	0.9959	0.23

Table 1. Comparative genotypic analysis of RSE02 and related type strains (based on whole genome sequence similarity). [1]digital DNA–DNA hybridization (dDDH) (calculated from the GGDC 2.1). [2]ANIb, ANIm (determined in JSpeciesWS).

the gastric environment and the presence of RSE02 in live form in the intestine are critical milestones in its potential as a probiotic[46]. This ability to traverse the digestive system positions RSE02 as a viable candidate for oral administration.

Effects of HFD and RSE02 on body weight gain in mice

The experimental data showed a significant increase in the body weight of HFD-fed mice compared to the untreated control (Fig. 6A–C). The initial weights of all mice were the same at the onset of the experiment. The body weight of HFD-fed mice gradually increased from 30 to 55 g until the end of the treatment period.

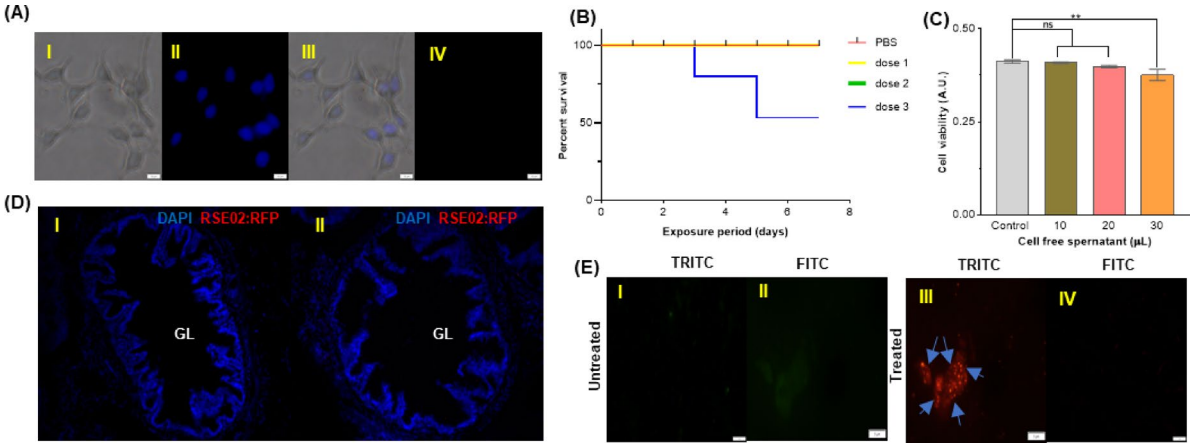

Fig. 5. (**A**I–IV) Cell adhesion assay of RFP-labelled RSE02 in Caco-2 cell line where, AI: Phase contrast, AII: DAPI staining, AIII: merge image of AI & AII and AIV: TRITC filter respectively under 40X magnification. (**B**) Kaplan-meir survival curve of zebrafish on exposure to RSE02 strain (PBS: Control, dose 1: 1×10^9 CFU/mL, dose 2: 1×10^{10} CFU/mL and dose 3: 2×10^{10} CFU/mL). (**C**) Cell cytotoxicity of Caco-2 cell line on exposure RSE02 bacterial cell free supernatant (control: PBS, 10, 20 and 30 µL csf: 1×10^9 CFU/mL bacteria. (**D**I & II) Transverse section of gut through the intestinal bulb segment showing RFP-labelled RSE02 (red) and nuclear DAPI staining (blue) in Control (PBS exposure) and RSE02-exposed adult zebrafish after 7 day treatment; GL, Gut lumen; Magnification 10x; Scale bar 100 µm. (**E**I–IV) Microscopic visualization RSE02 in zebrafish gut smear where, **E**I & II: gut smear of untreated fish under both TRITC & FITC filter and **E**III & IV: gut smear of treated fish under both TRITC & FITC filter.

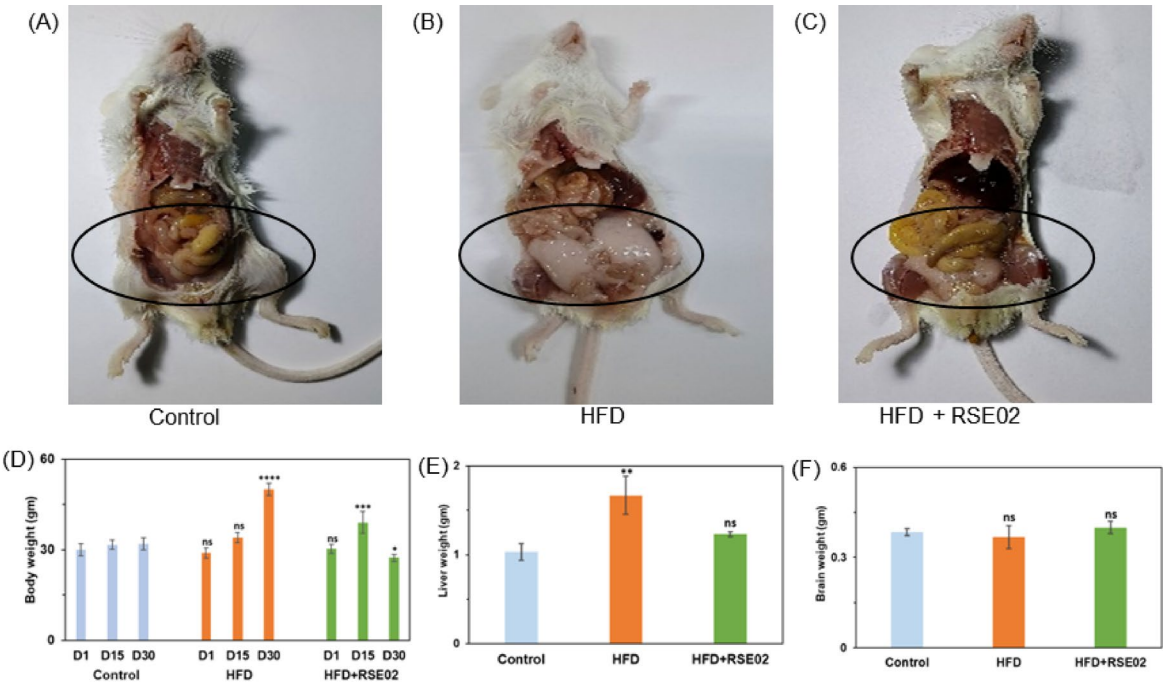

Fig. 6. Morphological study of mice. (**A**–**C**) Morphology of mice control, HFD and HFD + RSE02, respectively. (**D**) Body weight of day 1, day 15 and day 30 of control, HFD and HFD + RSE02 mice, respectively. (**E** & **F**) Liver and brain weight of control, HFD and HFD + RSE02 mice, respectively. All data were taken from three random measurment. Mean values in each column do not differ significantly at $p < 0.05$. Comparison between control and treatment mean values was made by Dunnett's multiple comparisons test. Where, "****" = $p < 0.0001$, "***" = $p < 0.001$, ""**" = $p < 0.01$, "*" = $p < 0.1$, "ns" = data is not significant. Data were subjected to analysis of variance (ANOVA ordinary one way) test.

In contrast, although the weight of RSE02-supplemented mice increased from 30 to 40 g on the 15th day (as the mice were already on HFD), but on the day 30th the weight was similar to that of the control mice. The weight of the livers of HFD mice increased notably, but upon treatment with RSE02, the liver weights became similar to those of the control mice. However, no significant changes in brain weight were observed among the experimental groups (Fig. 6D–F).

Effect of RSE02 on serum lipids

Using a murine model, it was found that the blood samples of HFD mice contained very high amounts of cholesterol. The enhanced cholesterol level in the blood of HFD mice was significantly reduced when the mice were fed with the probiotic RSE02. The serum lipid levels of the control and treated groups are presented in Fig. 7A–E. The HFD mice showed a significant increase in HDL LDL, VLDL, TG and cholesterol levels in serum, as compared to the control mice which are under normal diet indicating abnormality in lipid metabolizing machinery. Interestingly, the serum HDL, LDL, VLDL, and TG levels decreased to normal levels, similar to those of the control mice when treated with RSE02. The potential of RSE02 to mitigate hypercholesterolemia in mice establishes a direct link with cardiovascular health[47].

Effect of RSE02 on liver function

The levels of serum SGPT (or ALT) and SGOT (or AST), commonly indicating liver function, were analyzed, and the data are shown in Fig. 7F–M. Compared to untreated control mice, the serum levels of SGPT and SGOT were significantly increased in HFD mice, indicating an abnormal liver. Conversely, RSE02 supplementation markedly reduced the HFD-induced elevation of serum SGPT and SGOT, stimulated by HFD. The levels of CRP, bilirubin and alkaline phosphatase increased in obese mice and decreased after bacterial supplementation (Fig. 7F–J). However, the changes in the levels of blood albumin, globulin, and total protein remained insignificant among the three experimental sets (Fig. 7K–M).

Effect of RSE02 on oxidative stress in the liver

Protein content and different oxidative stress parameters, such as MDA and reduced GSH levels, along with catalase activity, were monitored to gauge the oxidative stress in the liver tissue of control and treated mice (Fig. 8A–D). The levels of GSH and MDA and the activity of antioxidant enzymes, such as catalase, were elevated in HFD-fed mice, which was significantly reduced by treatment with RSE02.

Histoarchitecture of liver and brain tissues

Histological observation of liver tissue showed normal architecture in the liver section of untreated control mice, while HFD-fed mice had micro and macro vesicular lipid deposition (steatosis) in the liver, and treatment with RSE02 reduced the numbers (Fig. 8E–G). Similarly, normal construction, composed of a clear granular layer, molecular layer, and white matter of brain tissue, was observed in untreated control mice, while only HFD-fed mice had vacuolated white matter, and in the case of RSE02 supplementation, the number of vacuolation decreased (Fig. 8H–M).

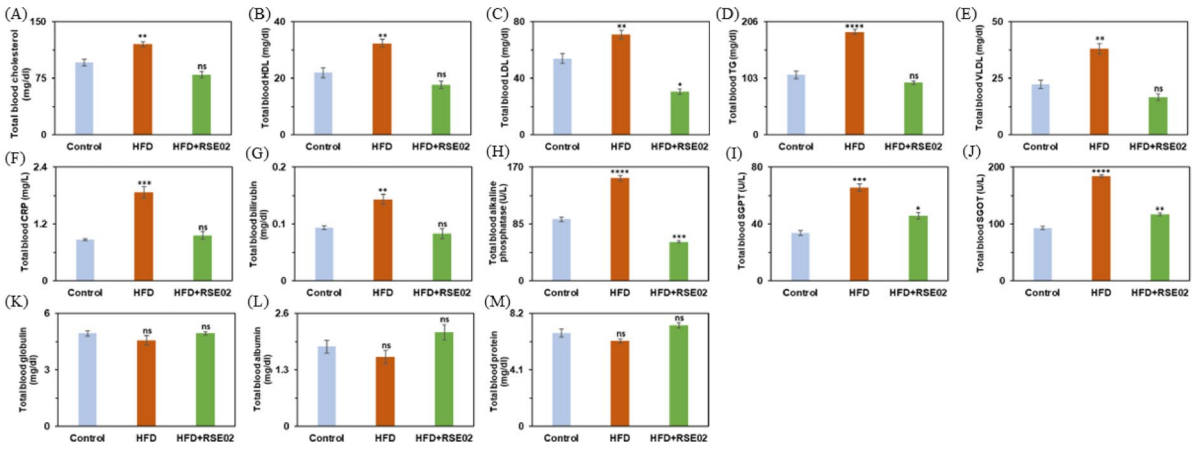

Fig. 7. Lipid profile and Liver Profile of Control, HFD and HFD + RSE02 mice. (**A**–**E**) Lipid profile (Total blood cholesterol, HDL, LDL, TG and VLDL) of Control, HFD and HFD + RSE02 mice respectively. (**F**–**M**) Liver profile (total blood CRP, bilirubin, alkaline phosphatase, SGPT, SGOT, globulin, albumin and protein) of Control, HFD and HFD + RSE02 mice, respectively. Mean (from three independent data point) values in each column do not differ significantly at $p < 0.05$. Comparison between control and treatment mean values was made by Dunnett's multiple comparisons test. Where, "****" = **p** < 0.0001, "***" = $p < 0.001$, ""**" = $p < 0.01$, "*" = $p < 0.1$, "ns" = data is not significant. Data were subjected to analysis of variance (ANOVA ordinary one way) test.

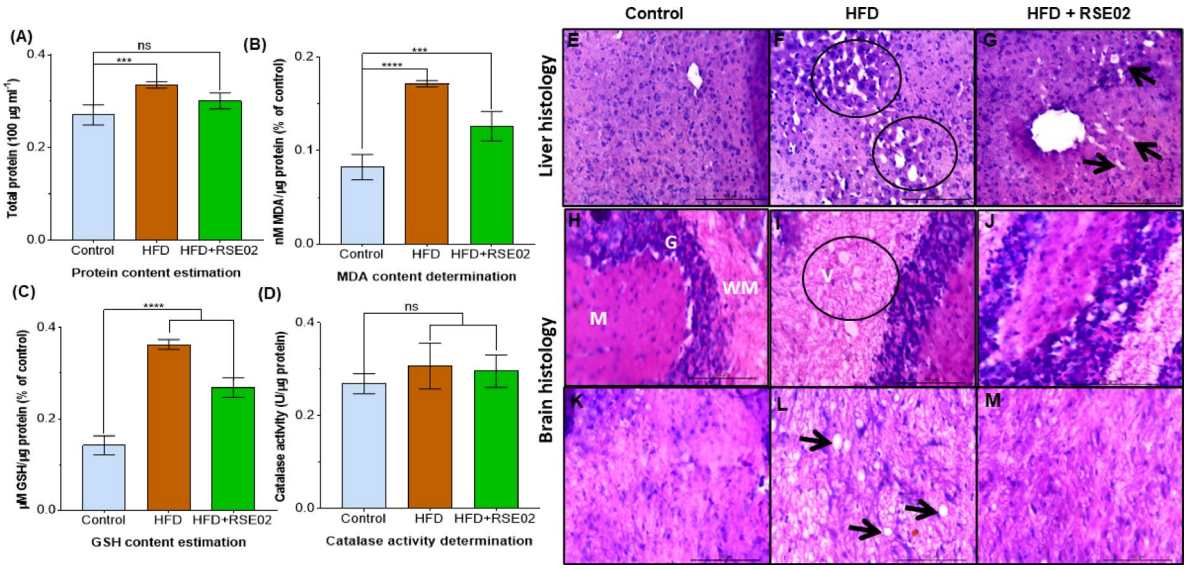

Fig. 8. Liver, Brain histology and Biochemical analysis of gut tissue of mice. (**A**–**D**) Biochemical analysis of total protein, MDA content, GSH content and catalase activity of gut tissue of mice, respectively. Mean values in each column do not differ significantly at $p < 0.05$. Comparison between control and treatment mean values was made by Dunnett's multiple comparisons test. Where, "****" = $p < 0.0001$, "ns" = data is not significant. Data were subjected to analysis of variance (ANOVA one way) test by using the GraphPad Prism 8.0.1 version software. (**E**) Control liver having normal hepatic lobules. (**F**) is the liver section of HFD fed mice having lipid deposition (black circle) in intracellular space of hepatic cells. (**G**) is the liver section of probiotic fed mice with almost normal histoarchitecture having reduced number of lipid droplets (arrow heads) than the former. (**H**) Control brain depicting clear granular layer (G), molecular layer (M) and white matter (WM); (**I**) brain tissue section of HFD fed mice is having vacuolated (V) white matter while in case of HFD + RSE02 fed mice brain. (**J**) the reduced size and numbers of vacuoles in white matter were observed. (K-M) are images of white matter of control, HFD fed and HFD + RSE02 fed mice, respectively where L is having vacuolated white matter but the condition became better in M.

Discussion

The findings of this study comprehensively highlight the multifaceted characteristics of *Phytobacter* sp. RSE02, a rice seed-derived endophyte, demonstrating significant potential as a plant- and human-beneficia; probiotic. These results have implications across agricultural and biochemical domains, encompassing its biochemical profile, survivability under gastrointestinal conditions, genomic attributes, immunomodulatory capacity, and its ability to modulate lipid metabolism and oxidative stress in mammalian models.

Biochemical features and agricultural implications

The notable biochemical features of RSE02 fall within the established criteria of probiotic strains[48]. This is particularly significant in the context of agriculture, where the application of probiotics can positively influence plant growth and combat soilborne fungal pathogens[2]. The observed plant growth promotion and biocontrol activities against fungal pathogens indicate the importance of RSE02 in sustainable agriculture[5]. The enhanced nutrient production and secretion of bioactive compounds suggest additional nutraceutical and therapeutic roles, opening avenues for the development of novel plant probiotics with broader applications[42].

The ability of RSE02 to survive in a GI-mimicked environment is a crucial trait for its potential as a probiotic. The GI tract possesses formidable challenges, particularly the acidic conditions of the stomach, which many bacteria struggle to withstand[41]. RSE02's robust survival in simulated gastric conditions indicates its potential to reach the intestines in a viable state, enabling it to exert its probiotic effects[49]. This survivability is a key factor in evaluating the feasibility of utilizing RSE02 as a beneficial microorganism in human health. The enhanced nutrient production and secretion of bioactive compounds point towards a broader spectrum of health-promoting effects[50]. The genomic analysis of RSE02 is pivotal in establishing its safety as a probiotic. The absence of virulence factors and the presence of genes associated with beneficial functions affirm its safety status[51]. This genomic characterization meets preliminary safety requirements for regulatory approval and leads to a safer use of RSE02 in various applications.

Safety profiles of RSE02

The finding that RSE02 does not adhere to the Caco2 cell line is noteworthy and challenges conventional notions of probiotic mechanisms. Adherence to intestinal epithelial cells is often considered a crucial step for probiotics in exerting their effects[44]. The lack of adherence in RSE02 suggests alternative mechanisms underlying its probiotic activities. This unique interaction pattern raises questions that warrant further investigation into the specific

pathways through which RSE02 influences host health and whether it employs unconventional mechanisms for establishing beneficial effects.

The evaluation of RSE02 for toxicity against human cell lines and zebrafish is a critical step in determining its safety for potential therapeutic applications[45]. The absence of cytotoxic effects in human cell lines and the non-toxicity to zebrafish affirm the safety profile of RSE02. These results are reassuring and provide confidence in considering RSE02 for further development as a probiotic strain with applications in human health.

Implications of RSE02 for human health

The ability of RSE02 to pass through the gastric environment and be present in live form in the intestine is a pivotal aspect of its potential as a probiotic[52]. Many bacteria face challenges surviving the acidic conditions of the stomach, and the successful passage of RSE02 through this environment is a testament to its resilience. The recovery of live bacteria from the intestine further supports its potential to establish an advantageous presence in the gut, where probiotic effects are often exerted[46]. The promising results demonstrating the ability of RSE02 to mitigate hypercholesterolemia in mice have direct implications for cardiovascular health interventions[47]. Further studies are warranted to elucidate the specific mechanisms through which RSE02 exerts its cholesterol-lowering effects and to explore its potential as a therapeutic agent in managing cardiovascular health.

Intake of a high-fat diet disrupts this balance leading to excessive accumulation of lipids, designated as hepatic steatosis, and subsequent oxidative stress condition causing liver damage[53]. In this context, the role of our lab-isolated RSE02 bacteria on obese mice liver was observed. Lipid accumulation was quantified by measuring the concentration of plasma TG, which rise significantly in livers of HFD-fed mice validating liver steatosis[54]. However, treatment with RSE02 substantially diminished the steatotic condition. Catalase is a potent antioxidant enzyme known to actively convert hydrogen peroxide into oxygen and water molecules, thus scavenging oxidative stress[55]. While the non-enzymatic antioxidant GSH can directly mitigate reactive oxygen species by readily conjugating with them[56]. Likewise, MDA is a terminal product of peroxidation of polyunsaturated fatty acid-mediated by free radicals[57]. Our results showed that oral administration of RSE02 mitigated oxidative stress induced by a high-fat diet, as evidenced by significantly reduced levels of MDA, GSH, and catalase activity compared to untreated controls. To further validate our findings, we measured serum SGPT and SGOT levels, which indicate damage in liver function[58]. The levels of serum SGPT and SGOT significantly decreased in RSE02 treatment which was augmented in HFD treatment alone, corroborating the finding of Liang et al. (2018)[59], where the probiotic mixture of *Lactobacillus* and *Bifidobacterium* reduced SGPT and SGOT levels in obese mice. Obesity is associated with increased levels of cholesterol, LDL, VLDL and decreased levels of HDL, leading to cardiovascular disease[60]. Our data showed that after completion of the experiment, cholesterol, LDL, and VLDL levels significantly escalated in HFD-fed mice, which were reduced by treatment with RSE02. Serum levels of bilirubin, albumin and alkaline phosphatase were also measured. Bilirubin is the terminal product of the heme metabolism in the liver, having endogenous antioxidant properties[61]. Serum albumin transports free fatty acids from source adipose tissue to different sink organs thus hike in albumin level leads to hepatic steatosis[62]. Similarly, alkaline phosphatase modulates fat deposition in intracellular tissue sites and in obesity the activity of this enzyme is increased subjecting to excess fat deposition[63]. Our data also depicts elevated levels of albumin and alkaline phosphatase in HFD-fed mice and the scenario became quite relieving by supplementation with our laboratory-isolated bacteria. To further validate this, we performed a histoarchitectural observation of liver and brain tissue. Intra or intercellular lipid deposition is a crucial indication of obesity[64,65]. Our data showed a large number of lipid vacuoles in the liver section of HFD-fed mice while the numbers were reduced in mice fed with bacterial supplementation. We also observed histoarchitecture of brain tissue as it is extremely sensitive and highly vulnerable to oxidative damage[66]. We observed necrotic spots and vacuolation in the brain tissue of obese mice which were consistent with data of Samad et al., 2023 [67], but the effect was minimized after bacterial treatment. In summary, our finding reveals simultaneous administration of RSE02 can minimize obesity-mediated fatal outcomes and thus can be used as a potential probiotic to deal with obesity.

Integrated insights and translational outlook

These findings collectively present RSE02 as a multifunctional probiotic strain with translational potential. Its dual functionality as a plant growth promoter and potential human probiotic supports the emerging concept of 'plant probiotics' that bridge agriculture and human health. The biochemical, genomic, and functional characterizations form a scientific basis for developing RSE02 into agricultural sustainability and human health applications.

Conclusion

In conclusion, this study highlights the promising potential of the rice seed endophytic bacterium *Phytobacter* sp. RSE02 as a plant probiotic with significant human health benefits. Our comprehensive biochemical and molecular analyses reveal that RSE02 not only promotes plant growth and suppresses phytopathogens but also exhibits remarkable probiotic characteristics relevant to human health, particularly its ability to reduce blood lipid levels. The time-dependent reduction in lipid accumulation observed in the blood, liver, peritoneal, and brain tissues of high-fat diet-induced obese mice underscores RSE02's potential as a natural lipid-lowering agent. This finding suggests that oral intake of RSE02, possibly through consumption of RSE02 colonized rice seeds, may contribute to the regulation of lipid metabolism and improved cardiovascular health. Future research should focus on elucidating the molecular mechanisms underlying RSE02's probiotic effects, particularly the genes and pathways involved in lipid metabolism and immune modulation. Exploring its application in personalized nutrition, accounting for individual microbiome variability, could unlock new avenues for targeted health interventions. Furthermore, interdisciplinary collaborations between agricultural and pharmaceutical sectors may facilitate the development of biofortified crops or next-generation probiotic formulations. This

works reinforces the emerging paradigm of leveraging beneficial plant-associated microbes for both agricultural sustainability and human health and positioned *Phytobacter* sp. RSE02 as a valuable model to pave the way for future innovations in this evolving field.

Data availability

The genome sequence data generated and analysed during the current study are available in the [NCBI] repository [https://www.ncbi.nlm.nih.gov/bioproject/PRJNA1127180] with the accession number PRJNA1127180. The other datasets used and/or analysed during the current study available from the corresponding author on reasonable request.

Received: 26 February 2025; Accepted: 8 July 2025
Published online: 30 July 2025

References

1. Compant, S., Duffy, B., Nowak, J., Clément, C. & Barka, E. A. Use of plant growth-promoting bacteria for biocontrol of plant diseases: Principles, mechanisms of action, and future prospects. *Appl. Environ. Microbiol.* **71**, 4951–4959 (2010).
2. Berg, G. Plant-microbe interactions promoting plant growth and health: Perspectives for controlled use of microorganisms in agriculture. *Appl. Microbiol. Biotechnol.* **84**, 11–18 (2009).
3. Muhammad, M. et al. Harnessing bacterial endophytes for environmental resilience and agricultural sustainability. *J. Environ. Manag.* **368**, 122201. https://doi.org/10.1016/j.jenvman.2024.122201 (2024).
4. El-Saadony, M. T. et al. Plant growth-promoting microorganisms as biocontrol agents of plant diseases: Mechanisms, challenges and future perspectives. *Front. Plant Sci.* **13**, 923880. https://doi.org/10.3389/fpls.2022.923880 (2022).
5. Jana, S. K., Islam, M. M., Hore, S. & Mandal, S. Rice seed endophytes transmit into the plant seedling, promote plant growth and inhibit fungal phytopathogens. *Plant Growth Regul.* **99**, 373–388. https://doi.org/10.1007/s10725-022-00914-w (2023).
6. Mendes, R. et al. Deciphering the rhizosphere microbiome for disease-suppressive bacteria. *Science* **332**, 1097–1100 (2011).
7. Pandey, S. S. et al. Plant probiotics–endophytes pivotal to plant health. *Microbiol. Res.* **263**, 127148. https://doi.org/10.1016/j.micres.2022.127148 (2022).
8. Verma, S. K. et al. Seed-vectored endophytic bacteria modulate development of rice seedlings. *J. Appl. Microbiol.* **122**, 1680–1691. https://doi.org/10.1111/jam.13463 (2017).
9. Jana, S. K., Islam, M. M. & Mandal, S. Endophytic microbiota of rice and their collective impact on host fitness. *Curr. Microbiol.* **79**, 37. https://doi.org/10.1007/s00284-021-02737-w (2022).
10. Islam, M. M., Jana, S. K., Sengupta, S. & Mandal, S. Impact of rhizospheric microbiome on rice cultivation. *Curr. Microbiol.* **81**, 188. https://doi.org/10.1007/s00284-024-03703-y (2024).
11. Rajendra Prasad, S. et al. Seed bio-priming for biotic and abiotic stress management. Microbial Inoculants in Sustainable Agricultural Productivity: Vol. 1: *Research Perspectives* 211–228 (2016). https://doi.org/10.1007/978-81-322-2647-5_12.
12. Davin-Regli, A. & Pagès, J. M. *Enterobacter aerogenes* and *Enterobacter cloacae*; versatile bacterial pathogens confronting antibiotic treatment. *Front. Microbiol.* **6**, 392. https://doi.org/10.3389/fmicb.2015.00392 (2015).
13. Krausova, G. et al. Identification of synbiotics conducive to probiotics adherence to intestinal mucosa using an in vitro Caco-2 and HT29-MTX cell model. *Processes* **9**, 569. https://doi.org/10.3390/pr9040569 (2021).
14. Wang, Y. et al. Whole-genome analysis of probiotic product isolates reveals the presence of genes related to antimicrobial resistance, virulence factors, and toxic metabolites, posing potential health risks. *BMC Genomics* **22**, 1–12. https://doi.org/10.1186/s12864-021-07539-9 (2021).
15. Nguyen, T. D. T., Kang, J. H. & Lee, M. S. Characterization of Lactobacillus plantarum PH04, a potential probiotic bacterium with cholesterol-lowering effects. *Int. J. Food Microbiol.* **113**, 358–366. https://doi.org/10.1016/j.ijfoodmicro.2006.08.015 (2007).
16. Patra, D., Pal, K. K. & Mandal, S. Inter-species interaction of bradyrhizobia affects their colonization and plant growth promotion in Arachis hypogaea. *World J. Microbiol. Biotechnol.* **40**, 1–16 (2024).
17. Meier-Kolthoff, J. P. & Göker, M. TYGS is an automated high-throughput platform for state-of-the-art genome-based taxonomy. *Nat. Commun.* **10**, 2182 (2019).
18. Lefort, V., Desper, R. & Gascuel, O. FastME 2.0: A comprehensive, accurate, and fast distance-based phylogeny inference program. *Mol. Biol. Evol.* **32**(10), 2798–2800. https://doi.org/10.1093/molbev/msv150 (2015).
19. Richter, M. & Rosselló-Mora, R. Shifting the genomic gold standard for the prokaryotic species definition. *Proc. Natl. Acad. Sci. USA* **106**, 19126–19131 (2009).
20. Richter, M., Rosselló-Mora, R., Glöckner, O. & Peplies, J. JspeciesWS: A web server for prokaryotic species circumscription based on pairwise genome comparison. *Bioinformatics* **32**, 929–931 (2016).
21. Meier-Kolthoff, J. P., Auch, A. F., Klenk, H. P. & Göker, M. Genome sequence-based species delimitation with confidence intervals and improved distance functions. *BMC Bioinform.* **14**, 1–14 (2013).
22. Avontuur, J. R. et al. Genome-informed Bradyrhizobium taxonomy: Where to from here?. *Syst. Appl. Microbiol.* **42**, 427–439 (2019).
23. Ormeño-Orrillo, E. & Martínez-Romero, E. A genomotaxonomy view of the Bradyrhizobium genus. *Front. Microbiol.* **10**, 450885 (2019).
24. Kanehisa, M. & Goto, S. KEGG: Kyoto encyclopedia of genes and genomes. *Nucleic Acids Res.* **28**, 27–30 (2000).
25. Grant, J. R. et al. Proksee: In-depth characterization and visualization of bacterial genomes. *Nucleic Acids Res.* **51**, W484–W492 (2023).
26. Somashekaraiah, R., Shruthi, B., Deepthi, B. V. & Sreenivasa, M. Y. Probiotic properties of lactic acid bacteria isolated from neera: A naturally fermenting coconut palm nectar. *Front. Microbiol.* **10**, 1382 (2019).
27. Kathade, S., Aswani, M. & Nirichan, B. Probiotic characterization and cholesterol assimilation ability of *Pichia kudriavzevii* isolated from the gut of the edible freshwater snail *Pila globosa*. *Egypt. J. Aquat. Biol. Fish.* **24**, 23–39 (2020).
28. Nath, S., Sikidar, J., Roy, M. & Deb, B. In vitro screening of probiotic properties of *Lactobacillus plantarum* isolated from fermented milk product. *Food Qual. Saf.* **4**, 213–223 (2020).
29. Manvelyan, A., Balayan, M., Miralimova, S., Chistyakov, V. & Pepoyan, A. Biofilm formation and auto-aggregation abilities of novel targeted aqua-probiotics. *Funct. Foods Health Dis.* **13**, 179–190 (2023).
30. Zhu, H. et al. Cholesterol-lowering effect of bile salt hydrolase from a *Lactobacillus johnsonii* strain mediated by FXR pathway regulation. *Food Funct.* **13**, 725–736 (2022).
31. Tomaro-Duchesneau, C. et al. Cholesterol assimilation by *Lactobacillus* probiotic bacteria: An in vitro investigation. *Biomed. Res. Int.* **2014**, 380316 (2014).
32. Mosmann, T. Rapid colorimetric assay for cellular growth and survival: Application to proliferation and cytotoxicity assays. *J. Immunol. Methods* **65**, 55–63 (1983).
33. Palaniyandi, S. A., Damodharan, K., Suh, J. W. & Yang, S. H. Probiotic characterization of cholesterol-lowering *Lactobacillus fermentum* MJM60397. *Probiotics Antimicrob. Proteins* **12**, 1161–1172 (2020).

34. Pham, L. N., Kanther, M., Semova, I. & Rawls, J. F. Methods for generating and colonizing gnotobiotic zebrafish. *Nat. Protoc.* **3**, 1862–1875 (2008).
35. Sheng, Y. et al. The presence or absence of intestinal microbiota affects lipid deposition and related gene expression in zebrafish (*Danio rerio*). *Front. Microbiol.* **9**, 1124 (2018).
36. Rawls, J. F., Samuel, B. S. & Gordon, J. I. Gnotobiotic zebrafish reveal evolutionarily conserved responses to the gut microbiota. *Proc. Natl. Acad. Sci. USA* **101**, 4596–4601 (2004).
37. Santos, R. A. et al. Bacillus spp. inhibit Edwardsiella tarda quorum-sensing and fish infection. *Mar. Drugs* **19**, 602 (2021).
38. Beutler, E. Improved method for the determination of blood glutathione. *J. Lab. Clin. Med.* **61**, 882–888 (1963).
39. Aebi, H. Catalase in vitro. *Methods Enzymol.* **105**, 121–126. https://doi.org/10.1016/s0076-6879(84)05016-3 (1984).
40. Buege, J. A. & Aust, S. D. Microsomal lipid peroxidation. *Methods Enzymol.* **52**, 302–310 (1978).
41. Ogunbanwo, S. T., Sanni, A. I. & Onilude, A. A. Characterization of bacteriocin produced by *Lactobacillus plantarum* F1 and *Lactobacillus brevis* OG1. *Afr. J. Biotechnol.* **2**, 219–227 (2003).
42. Gaggìa, F., Mattarelli, P. & Biavati, B. Probiotics and prebiotics in animal feeding for safe food production. *Int. J. Food Microbiol.* **141**, S15–S28 (2010).
43. Ventura, M. et al. Comparative analyses of prophage-like elements present in bifidobacterial genomes. *Appl. Environ. Microbiol.* **75**, 6929–6936 (2009).
44. Ouwehand, A. C., Salminen, S. & Isolauri, E. Probiotics: An overview of beneficial effects. *Antonie Van Leeuwenhoek* **82**, 279–289 (2002).
45. Urdaci, M. C., Bressollier, P., Pinchuk, I. & Segura-Roggero, I. Modulation of *Helicobacter hepaticus* infection in mice following concurrent infection with *Lactobacillus*. *Microbiol. Immunol.* **48**, 187–195 (2004).
46. Mack, D. R. et al. Probiotics inhibit enteropathogenic *E. coli* adherence in vitro by inducing intestinal mucin gene expression. *Am. J. Physiol.* **276**, G941–G950 (1999).
47. Jones, M. L., Martoni, C. J. & Prakash, S. Cholesterol lowering and inhibition of sterol absorption by *Lactobacillus reuteri* NCIMB 30242: A randomized controlled trial. *Eur. J. Clin. Nutr.* **68**, 1302–1304 (2014).
48. Reid, G. et al. New scientific paradigms for probiotics and prebiotics. *J. Clin. Gastroenterol.* **52**, S6–S12 (2018).
49. Corsetti, A. & Settanni, L. Lactic acid bacteria in sourdough fermentation. *Food Res. Int.* **40**, 539–558 (2007).
50. Patel, A. K. & Denning, P. W. Therapeutic use of prebiotics, probiotics, and postbiotics to prevent necrotizing enterocolitis: What is the current evidence?. *Clin. Perinatol.* **40**, 11–25 (2013).
51. Wassenaar, T. M. & Zimmermann, K. Lipopolysaccharides in food, food supplements, and probiotics: should we be worried?. *Eur. J. Microbiol. Immunol.* **8**, 63–69 (2018).
52. Marteau, P. & Seksik, P. Tolerance of probiotics and prebiotics. *J. Clin. Gastroenterol.* **38**, S67–S69 (2004).
53. Friedman, S. L., Neuschwander-Tetri, B. A., Rinella, M. & Sanyal, A. J. Mechanisms of NAFLD development and therapeutic strategies. *Nat. Med.* **24**, 908–922 (2018).
54. Liou, C. J. et al. Protective effects of licochalcone A ameliorates obesity and non-alcoholic fatty liver disease via promotion of the Sirt-1/AMPK pathway in mice fed a high-fat diet. *Cells* **8**, 447 (2019).
55. Borrelli, A. et al. Role of gut microbiota and oxidative stress in the progression of non-alcoholic fatty liver disease to hepatocarcinoma: Current and innovative therapeutic approaches. *Redox Biol.* **15**, 467–479 (2018).
56. Krumschnabe, G. & Nawaz, M. Acute toxicity of hexavalent chromium in isolated teleost hepatocytes. *Aquat. Toxicol.* **70**, 159–167 (2004).
57. Smriti, K., Pai, K. M., Ravindranath, V. & Pentapati, K. C. Role of salivary malondialdehyde in assessment of oxidative stress among diabetics. *J. Oral Biol. Craniofac. Res.* **6**, 42–45 (2016).
58. Zhao, L. et al. Protective effects of *Lactobacillus plantarum* C88 on chronic ethanol-induced liver injury in mice. *J. Funct. Foods* **35**, 97–104 (2017).
59. Liang, Y. et al. Probiotic mixture of *Lactobacillus* and *Bifidobacterium* alleviates systemic adiposity and inflammation in non-alcoholic fatty liver disease rats through Gpr109a and the commensal metabolite butyrate. *Inflammopharmacology* **26**, 1051–1055 (2018).
60. Kotsis, V. The diabetic/obese hypertensive patient (including metabolic syndrome). *Manual of Hypertension of the European Society of Hypertension, Third Edition*, 417–423 (2019).
61. Inoguchi, T., Sonoda, N. & Maeda, Y. Bilirubin as an important physiological modulator of oxidative stress and chronic inflammation in metabolic syndrome and diabetes: A new aspect on old molecule. *Diabetol. Int.* **7**, 338–341 (2016).
62. Abdollahi, A. et al. Albumin deficiency reduces hepatic steatosis and improves glucose metabolism in a mouse model of diet-induced obesity. *Nutrients* **15**, 2060 (2023).
63. Ali, A. T., Paiker, J. E. & Crowther, N. J. The relationship between anthropometry and serum concentrations of alkaline phosphatase isoenzymes, liver enzymes, albumin, and bilirubin. *Am. J. Clin. Pathol.* **126**, 437–442 (2006).
64. Liu, L., Gao, C., Yao, P. & Gong, Z. Quercetin alleviates high-fat diet-induced oxidized low-density lipoprotein accumulation in the liver: Implication for autophagy regulation. *Biomed. Res. Int.* **2015**, 607531 (2015).
65. Patel, R. et al. Effect of dietary advanced glycation end products on mouse liver. *PLoS ONE* **7**, e35143 (2012).
66. Ganji, A., Salehi, I., Nazari, M., Taheri, M. & Komaki, A. Effects of *Hypericum scabrum* extract on learning and memory and oxidant/antioxidant status in rats fed a long-term high-fat diet. *Metab. Brain Dis.* **32**, 1255–1265 (2017).
67. Samad, N. et al. Protective effects of niacin following high fat rich diet: An in vivo and in silico study. *Sci. Rep.* **13**, 21343 (2023).

Acknowledgements

None.

Author contributions

Santosh Kumar Jana: Writing—original draft, Writing—review & editing, Visualization, Methodology. Rajarshi Bhattyacharya: Writing—original draft, Writing—review & editing, Visualization, Methodology. Sunanda Mukherjee: Writing—review & editing, Methodology. Samudra Gupta: Visualization, Methodology. Subhra Prakash Hui: Writing—review & editing, Methodology, Conceptualization. Ansuman Chattopadhyay: Methodology. Swadesh Ranjan Biswas: Methodology, Writing—review & editing. Sukhendu Mandal: Conceptualization, Methodology, Writing—review & editing.

Funding

There is no financial support for this research.

Declarations

Competing interests
The authors declare no competing interests.

Ethical approval
All experimental protocols involving mice were conducted in accordance with the ethical standards approved by the IACUC of Visva-Bharati University (Approval Number: IAEC/VB/2022-IV/06). Both the zebrafish and mice studies is reported in accordance with the ARRIVE guidelines.

Consent of publication
The data used for the manuscript is original and does not require any consent from third party for publication.

Additional information
Correspondence and requests for materials should be addressed to S.R.B. or S.M.

Reprints and permissions information is available at www.nature.com/reprints.

Publisher's note Springer Nature remains neutral with regard to jurisdictional claims in published maps and institutional affiliations.